

Insight of cleaning, doping and defective effects on the graphene surface by using methanol

Krishna Bahadur Rai*¹, Ishwor Bahadur Khadka²,
Agni Raj Koirala³ and Schindra Kumar Ray**⁴

¹ Department of Physics, Patan Multiple Campus, Tribhuvan University, Nepal

² Department of Physics, Sungkyunkwan University, Suwon 16419, Republic of Korea

³ Korea Center for Artificial Photosynthesis, Department of Chemistry,
Sogang University, Seoul 121-742, Republic of Korea

⁴ Department of Environment and Energy, Sejong University, Seoul 143-747, Republic of Korea

(Received July 13, 2020, Revised February 22, 2021, Accepted September 9, 2021)

Abstract. Graphene has attracted enormous interest to researchers because of its remarkable electrical, mechanical, and optical properties. Chemical vapor deposition (CVD) method was used to synthesize the graphene. The methanol (CH₃OH) was used to investigate the cleaning, doping and defective effect in the graphene surface. The samples were characterized by X-ray diffraction patterns (XRD), field emission scanning electron microscope (FESEM) images, X-ray photoelectron spectroscopy (XPS) measurements, and Raman spectroscopy. XRD indicates the introduction of oxygen in graphene layer. FESEM images of samples suggest the sheet like morphology. XPS measurements confirm the existence of large number of oxygen containing functional groups (C=O, COOH, and C-O) and C-C in the graphene surface. The Raman spectra confirm the n-doping and cleaning effects on graphene surface through the red shifts of G and 2D peaks. Furthermore, the optical images were used to observe the residues in graphene. The residues are obtained due to adsorption of CH₃OH in graphene surface. Therefore, this work provides a simple and effective approach to investigate the cleaning, doping and defective effects on the surface of graphene using CH₃OH solvent that can be applied in tunable electronic devices and gas sensor.

Keywords: defective effects; graphene; methanol; n-doping

1. Introduction

Graphene, one atomic thick layer of carbon atoms, has outstanding mechanical, electronic and chemical properties for future application (Geim and Novoselov 2009, Tiwari *et al.* 2020, Wong *et al.* 2019) It has wide application research areas such as energy, environment, medicine, electronics, light processing, sensors etc. Since past decades, several methods have been applied for synthesis of grapheme (Berger *et al.* 2004, Li *et al.* 2009a, Liu *et al.* 2017, Taghioskoui 2009). Among them, mechanical exfoliation process is employed for synthesis of high-quality grapheme. However, such type of process fails to fabricate the large area uniform monolayer graphene (Novoselov 2004). So, chemical vapor deposition (CVD) method is perfect choice to grow graphene on metal

*Corresponding author, Ph.D., E-mail: schindrakumarray@gmail.com

foils such as nickel or copper substrate (Lee *et al.* 2010). However, the formation of polymethyl methacrylate

(PMMA) residue as well defects are occurred during chemical treatment and transfer processes in CVD synthesis that makes low quality of graphene (Li *et al.* 2009b, Liang *et al.* 2011, Lin *et al.* 2011). However, grapheme/PMMA composites has effect of laminate configuration on the free vibration (Zeverdejani and Beni 2020). Defects and residues formed during the chemical treatment and transfer process can degrade the quality of graphene and modifies all the properties based on this material. So, the researchers are searching a new way to clean the residues and remove the defects as well as better transfer process on desired substrates. Ultra-clean and defect-free transfer of CVD graphene on the desired substrates is essential for its application in the electronic and other devices (Kang *et al.* 2012).

Nowadays, several solvents are used to remove PMMA. Among solvents, acetone is widely used to clean PMMA on graphene surface. However, it produces chemical contamination in graphene. p-doped occurred during this process (Suk *et al.* 2013). There are other many methods reported such as irradiation and heat treatment to make clean removal of PMMA (Cheng *et al.* 2011, Lin *et al.* 2011, Pirkle *et al.* 2011). However, obtaining better removal of residues, defective effect and n-doped CVD graphene simultaneously is problematic. So, we present a simple chemical treatment method in which methanol (CH₃OH) is the best choice to clean the residues and removing the defect effectively. It caused n-doped in graphene. In addition, transfer of graphene on hydrophobic film makes the reduction of defects (Rai *et al.* 2018). So, utilization of CH₃OH in CVD synthesized graphene is perfect way to investigate the cleaning, doping and defective effects on the graphene surface. In this article, CH₃OH is used to observe the cleaning effect, n-doping and defects in graphene surface. Raman spectra is employed to see these effects on graphene surface. Furthermore, the samples were well characterized by X-ray diffraction patterns (XRD), field emission scanning electron microscope (FESEM) images, and X-ray photoelectron spectroscopy (XPS) measurements.

2. Experiment details

Graphene was synthesized on poly-crystal copper foils (25 μm thick, Alfa-Aesar) in a rapid thermal processing chemical vapor deposition (CVD) chamber. The typical sample size having few cm² Cu foil was loaded into the CVD growth reactor and pumped to the base vacuum pressure (about 10⁻² Torr). The schematic presentation of the temperature versus time curve for the synthesis of CVD graphene has been shown in Fig. 1. Then, the CVD chamber was heated by allowing only Argon (Ar) gas (99 sccm – standard cm³/min) till the temperature reached 950°C (point 1 in Fig. 1) and then it was again adjusted to reach the temperature 1020°C (point 3). During the temperature rising from 950°C to 1020°C, the Hydrogen (H₂) gas (99 sccm) was started to pass at around 1003°C temperature for 1 h into the hot chamber. After 1 h cleaning with H₂ gas (point 2 to point 4), methane (CH₄) gas at the flow rate 21 sccm was passed (point 4) for 15 min at around 9.7 Torr pressure to carry out the graphene growth. Finally, the sample was cooled rapidly from point 5 (at 1020°C) to point 6 (at 725°C) then from point 6, the slow cooling process occurs at room temperature under Argon (Ar) ambient atmosphere.

The copper foil was etched using ferric chloride (FeCl₃) after spin coating with poly methyl methacrylate (PMMA). Then this PMMA/graphene was rinsed with deionized (DI) water more than five times (for approximately 30 min each). The PMMA/graphene samples were transferred

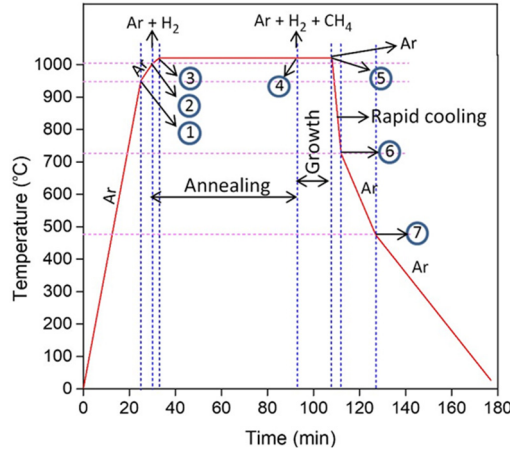


Fig. 1 Schematic presentation of the CVD graphene synthesis procedure showing operating conditions, time, temperature, gas flow and growth of graphene film. (point 1: 950°C, point 2: 1003°C, point 3: 1020°C, point 4: graphene growth, point 5: methane/hydrogen gas turn off, and point 6: cooling process)

on to a bare SiO₂/Si wafer with a 300 nm thick SiO₂ film and the PMMA film was removed by immersing the samples into acetone for 30 minutes. For cleaning and chemical doping, the samples were dipped into the methanol (99.9% purity) for 2 h, 4 h, 6 h, 8 h, 10 h, and 12 h. Fig. 2 shows the flowchart describing the experimental details for the CVD graphene, its doping with methanol and characterization. Raman Spectra (Inviva, 50 X objective, 1800 lines/mm grating, and 532 nm excitation laser source) is used to observe the charge impurities effects and disorder on graphene.

The XRD patterns of samples were taken on a Rigaku D/MAX-2500/pc diffractometer with Cu-Kα radiation. FESEM (JEOL JEM 7600) was used to see the morphology of samples. XPS measurements of samples were obtained by Axis Ultra DLD spectrometer (Kratos Analytical with a monochromatic Al Ka X-ray source at 150 W). All the samples were mounted using double-sided adhesive Carbon tape during XPS measurements.

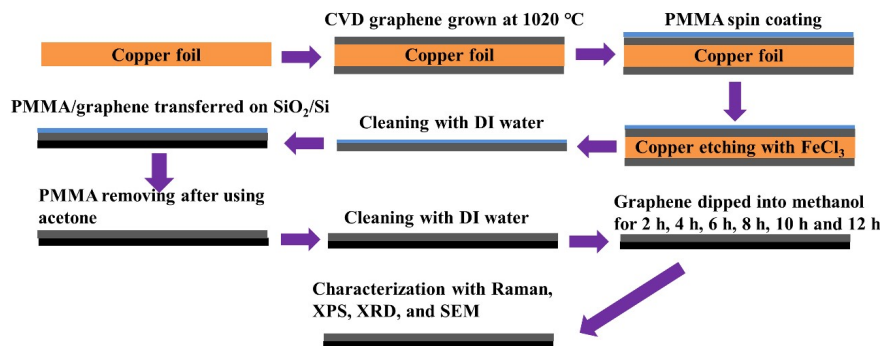


Fig. 2 Flowchart describing the experimental details for the CVD graphene, its doping with methanol and characterization

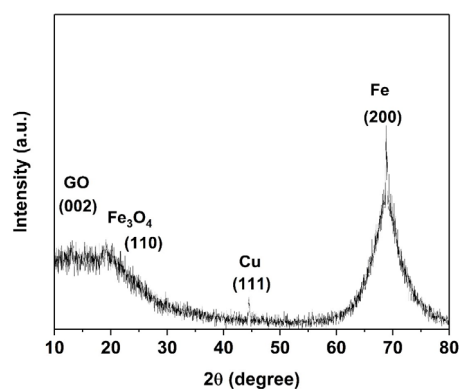


Fig. 3 XRD patterns of CVD synthesized graphene for 8 h dipping time in CH_3OH

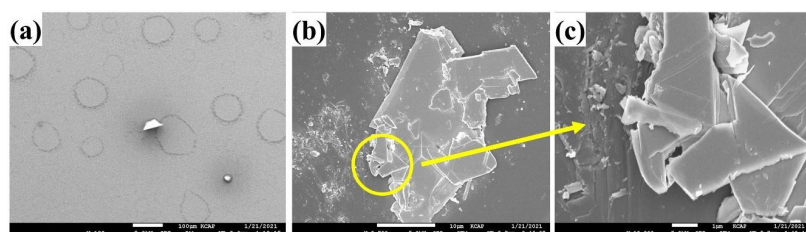


Fig. 4 FESEM images of graphene samples. (a) 0 h; (b) 8 h; and (c) magnified portion of (b)

3. Results and discussion

Fig. 3 represents XRD patterns of graphene sample containing CH_3OH for 8 h dipping time. The sample shows the diffraction peaks centered at 12.9° (002 plane) which reveals the formation of graphene oxide (GO) (Ibrahim *et al.* 2016). The possible reasons for formation of GO from graphene may associated with introduction of oxygen in graphene layer (Jeong *et al.* 2008). Furthermore, the diffraction peaks are appeared at 19.19° , 44.37° , and 68.81° that show the existence of Fe_3O_4 , Cu, and Fe, respectively (Narayanaswamy *et al.* 2019, Qu *et al.* 2014). It suggests the presence of residual oxidizing impurities during synthesis of graphene by CVD process (Reckinger *et al.* 2013). FESEM images of samples at 0 h, 2 h, and 8 h are displayed in Fig. 4. These images clearly indicate the sheet like morphology. As shown in Fig. 4(a), the graphene sheet at 0 h has a size about $70\ \mu\text{m}$. However, the samples at 2 h and 8 h have smaller size ($1\text{--}5\ \mu\text{m}$) than 0 h sample (Figs. 4(b) and 4(c)). These microsheets were agglomerated.

Fig. 5 presents the XPS spectra of graphene samples at 0 h, 2 h, and 8 h. The C 1s spectrum of graphene sample is deconvoluted contains into two peaks in 0 h (C-C: 283.31 eV and C-O: 286.61 eV), 2 h (C-C: 283.14 eV and C-O: 286.79 eV), and 8 h (C-C: 283.05 eV and C-O: 284.83 eV) samples (Figs. 5(a), 5(b), and 5(c)) (Johra *et al.* 2014). In addition, O 1s peaks are found in 0 h (C=O: 530.41 eV), 2 h (C=O: 530.21 eV and (CO)OH: 532.01 eV), and 8 h (C=O: 530.33 eV and (CO)OH: 531.65 eV) samples (Figs. 5(d), 5(e), and 5(f)) (Kwan *et al.* 2015). These XPS graph confirms the presence of large number of oxygen containing functional groups (C=O, COOH, and C-O) and C-C in the graphene surface.

Fig. 6(a). shows the Raman spectra of single layer graphene before (0 h) and after (2 h, 4 h, 6 h,

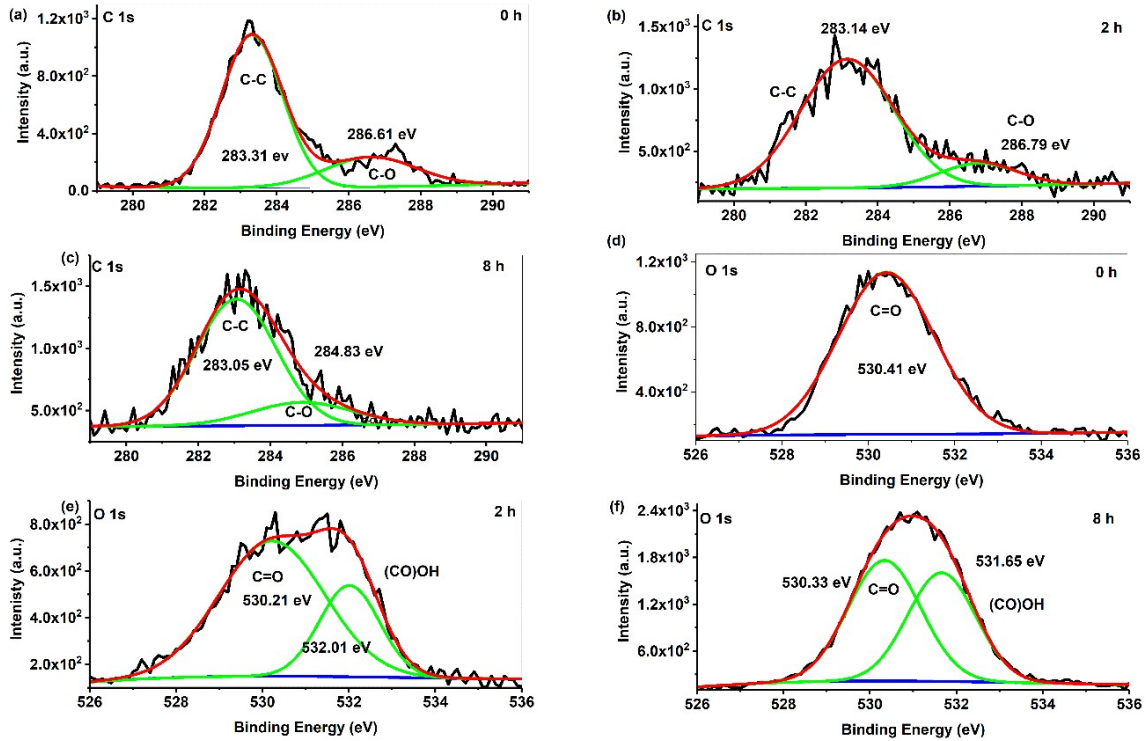


Fig. 5 XPS of samples at 0 h ((a) C 1 s and (d) O 1s) 2 h ((b) C 1 s and (e) O 1 s), and 8 h ((c) C 1 s and (f) O 1 s)

8 h, 10 h, and 12 h) doping with CH_3OH as prepared samples. The Raman spectra consist of G and D peaks at 1593 cm^{-1} and 1342 cm^{-1} respectively before doping. The G (E_{2g} mode) and D (Defect mode) peaks in Raman spectra indicate stretching plane of the $\text{C}=\text{C}$ bonds (sp^2 hybridized) and breathing modes of sp^2 atoms of the graphitic crystalline carbon atoms, respectively (Thomsen and Reich 2000). Likewise, 2D peak was observed at 2682 cm^{-1} at 0 h. This peak shows the existence of graphene in sample, which is originated from the second order double resonance process (Thomsen and Reich 2000). Figs. 6(b) and 6(c) reveal a clear red shift of Raman spectra after every 2 h of the methanol treatment. The red shift of the G and 2D peaks in CH_3OH treatment process makes an increase of electron density in the single layer grapheme (Wu *et al.* 2017). So, the presence of graphene in CH_3OH shows n-doped feature.

To find out the doping effect in Raman spectra, the I_{2D}/I_G intensity was calculated (Fig. 6(d)).

The I_{2D}/I_G intensity ratios of synthesized graphene sample was found to be 2.02 ± 0.06 , 2.07 ± 0.04 , 2.21 ± 0.04 , 2.25 ± 0.03 , 2.24 ± 0.03 , 2.15 ± 0.02 and 2.12 ± 0.06 for 0 h, 2 h, 4 h, 6 h, 8 h, 10 h, and 12 h respectively. In single layer grapheme, the ratio of the intensity of the 2D and G peaks (I_{2D}/I_G) is maximum for zero doping and decreases for increasing doping (Berciaud *et al.* 2010, Ferrari *et al.* 2006). It clearly suggests that the I_{2D}/I_G intensity ratio increases from 0 h to 6 h (no doping) and decreases after 6 to 12 h (doping). This gives the evidence about the cleaning of graphene surface and doping effect by using methanol solvent depending on different time variation of sample dipped. As shown in Fig. 6(a), the graphene on SiO_2/Si reveals strong D band peak before doping. This D band peak decreases gradually as the sample is dipped into CH_3OH for

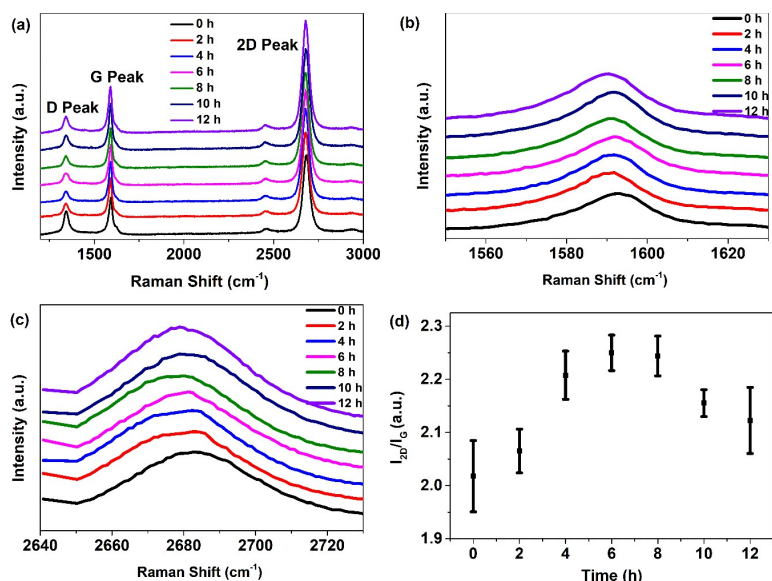


Fig. 6 Raman spectra of samples. (a) CVD graphene/SiO₂ with varying doping time; (b) G peak redshift of graphene doped with methanol; (c) 2D peak redshift of graphene doped with methanol; (d) the change of I_{2D}/I_G ratio of doped graphene with respect to change in time. The I_{2D}/I_G intensity ratio for 0 h, 2 h, 4 h, 6 h, 8 h, 10 h and 12 h are 2.02 ± 0.06 , 2.07 ± 0.04 , 2.21 ± 0.04 , 2.25 ± 0.03 , 2.24 ± 0.03 , 2.15 ± 0.02 and 2.12 ± 0.06 , respectively

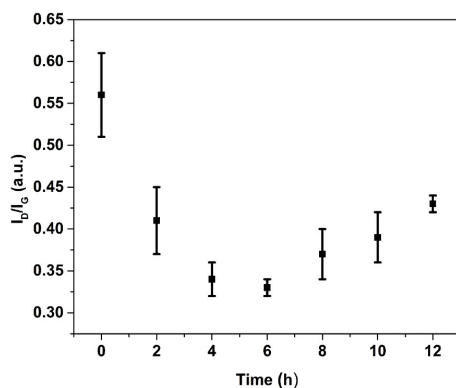


Fig. 7 The change of I_D/I_G ratio of defected graphene with respect to change in time. The I_D/I_G ratios for 0 h, 2 h, 4 h, 6 h, 8 h, 10 h, and 12 h are 0.56 ± 0.05 , 0.41 ± 0.04 , 0.34 ± 0.02 , 0.33 ± 0.01 , 0.37 ± 0.03 , 0.39 ± 0.03 and 0.43 ± 0.01 , respectively

2 h, 4 h, and 6 h. In addition, it increases after 8 h, 10 h, and 12 h. However, the G band intensity almost remains constant with different time (8 h, 10 h, and 12 h) doping.

The D band in graphene is strongly associated with the disorder. The increase in the intensity of I_D/I_G ratios indicate an increase in impurities and the measurement of the number of defects in graphitic materials (Goniszewski *et al.* 2015, Pimenta *et al.* 2007). These defects might be the number of small blisters residues of methanol and sublattice symmetry breaking caused by adsorption on graphene (Schröder 2013). To find the defects and impurities in graphene, the I_D/I_G

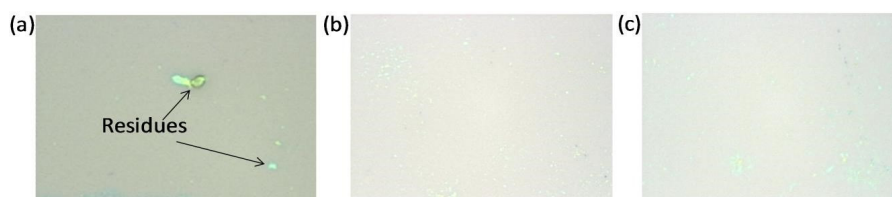


Fig. 8 optical images of samples. (a) Optical image of graphene with some residues before doping with methanol; (b) optical image of graphene after 2 h doping with methanol; and (c) after 8 h doping. There are still some blisters residues on graphene even after cleaning

ratios were calculated (Fig. 7).

The I_D/I_G intensity ratios were observed to be 0.56 ± 0.05 , 0.41 ± 0.04 , 0.34 ± 0.02 , 0.33 ± 0.01 , 0.37 ± 0.03 , 0.39 ± 0.03 and 0.43 ± 0.01 for 0 h, 2 h, 4 h, 6 h, 8 h, 10 h, and 12 h, respectively. This I_D/I_G value decreases with the increase of time up to 6 h for graphene dipped into CH_3OH . It suggests the enhancement of graphene quality by removing defects and cleaning impurities. I_D/I_G increases after 6 h because of formation of defects. The possible reason of defect may associate with that of dissociation of attached hydrogen atoms by graphene into incommensurate structure like turbostratic graphite which behaves like a defect (Kim *et al.* 2012). These defects in the hydrogenated graphene are caused by the formation of sp^3 C-H bonds as well as the breaking of the translational symmetry of sp^2 C=C network (Bae *et al.* 2012). The graphene with such Hydrogen atom as impurities is considered of n-doping effect (Kim *et al.* 2012).

The transition metals like Cu and Fe remaining on graphene makes the methanol decomposition proceeding through the successive formation of methoxy, formaldehyde, formyl into CO and hydrogen in which CO would be expected to be more soluble in CH_3OH than H_2 at room temperature (Mavrikakis and Barteau 1998). To analyze the formation of residual contamination during the growth process before and after doping in graphene, optical images of graphene were taken (Fig. 8). The optical images suggest the existence of a small number of blisters residues after doping with CH_3OH . These blisters residues (defective effects) are associated with thin film of bi-layer and multilayer of CH_3OH (Wang *et al.* 2002). Agglomeration of trace number of elements (Fe, Cu) during the etching process and generation of Fe or Cu elements during PMMA assisted wet chemical transfer process are also responsible for formation of blister residues. Furthermore, the comparison of this work with other similar published reports have been presented in Table 1.

Table 1 The comparison of this work with other similar reports

Materials	Synthesis methods	Results	Ref.
Graphene	Mechanical exfoliation	Cleaning of graphene by using AFM and improvement of charge neutrality	(Lindvall <i>et al.</i> 2012)
PMMA, acetone, and graphene	CVD	Cleaning of graphene by heat treatment	(Park <i>et al.</i> 2013)
Graphene and CH_3OH	Microwave plasma enhanced CVD	Efficient methanol oxidation	(Soin <i>et al.</i> 2011)
Graphene and CH_3OH	CVD graphene	Cleaning, n-doped graphene, and blisters residues as defective effects	Our work

4. Conclusions

In this paper, we demonstrate the synthesis of graphene by using CVD process. CH₃OH is used to clean the sheet like morphology of graphene surface. The formation of oxygen in graphene was confirmed by XRD analysis. Oxygens containing functional groups (C=O, COOH, and C-O) and C-C in the graphene surface was proved by XPS measurements. The Raman spectra of single layer graphene shows the G, D, and 2D peaks. The red shift of the G and 2D peaks during CH₃OH treatment was analyzed by Raman Spectra and calculating the I_{2D}/I_G intensity ratios that clearly suggest the cleaning of graphene surface and doping phenomena. Likewise, I_D/I_G intensity ratios indicate the removal of defect and impurity in graphene surface. Moreover, CH₃OH dipped graphene shows the n-type nature. Optical images of graphene confirm the improvement of cleaning process in graphene surface by using CH₃OH. In conclusion, CH₃OH solvent is promising solvent to see the cleaning, doping and defective effects on the surface of graphene. Such type of promising materials can be applied in wide range of applications CVD synthesized graphene can be used in microelectronics, coating, sensor, devices, and energy storage.

References

- Bae, G., Cha, J., Lee, H., Park, W. and Park, N. (2012), "Effects of defects and non-coordinating molecular overlayers on the work function of graphene and energy-level alignment with organic molecules", *Carbon*, **50**, 851-856. <https://doi.org/10.1016/j.carbon.2011.09.044>
- Berciaud, S., Han, M.Y., Mak, K.F., Brus, L.E., Kim, P. and Heinz, T.F. (2010), "Electron and optical phonon temperatures in electrically biased graphene", *Phys. Rev. Lett.*, **104**, 2-5. <https://doi.org/10.1103/PhysRevLett.104.227401>
- Berger, C., Song, Z., Li, T., Li, X., Ogbazghi, A.Y., Feng, R., Dai, Z., Alexei, N., Conrad, M.E.H., First, P.N. and De Heer, W.A. (2004), "Ultrathin epitaxial graphite: 2D electron gas properties and a route toward graphene-based nanoelectronics", *J. Phys. Chem. B*, **108**, 19912-19916. <https://doi.org/10.1021/jp040650f>
- Cheng, Z., Zhou, Q., Wang, C., Li, Q., Wang, C. and Fang, Y. (2011), "Toward intrinsic graphene surfaces: A systematic study on thermal annealing and wet-chemical treatment of SiO₂-supported graphene devices", *Nano Lett.*, **11**, 767-771. <https://doi.org/10.1021/nl103977d>
- Ferrari, A.C., Meyer, J.C., Scardaci, V., Casiraghi, C., Lazzeri, M., Mauri, F., Piscanec, S., Jiang, D., Novoselov, K.S., Roth, S. and Geim, A.K. (2006), "Raman spectrum of graphene and graphene layers", *Phys. Rev. Lett.*, **97**, 1-4. <https://doi.org/10.1103/PhysRevLett.97.187401>
- Geim, A.K. and Novoselov, K.S. (2009), *The rise of graphene, in: Nanoscience and Technology*, Macmillan Publishers Ltd., UK, pp. 11-19. https://doi.org/10.1142/9789814287005_0002
- Goniszewski, S., Gallop, J., Adabi, M., Gajewski, K., Shaforost, O., Klein, N., Sierakowski, A., Chen, J., Chen, Y., Gotszalk, T. and Hao, L. (2015), "Self-supporting graphene films and their applications", *IET Circuits, Devices Syst.*, **9**, 420-427. <https://doi.org/10.1049/iet-cds.2015.0149>
- Ibrahim, I., Lim, H.N., Huang, N.M. and Pandikumar, A. (2016), "Cadmium sulphide-reduced graphene oxidemodified photoelectrode-based photoelectrochemical sensing platform for copper(II) ions", *PLoS One*, **11**, 1-18. <https://doi.org/10.1371/journal.pone.0154557>
- Jeong, H.K., Yun, P.L., Lahaye, R.J.W.E., Park, M.H., Kay, H.A., Ick, J.K., Yang, C.W., Chong, Y.P., Ruoff, R.S. and Young, H.L. (2008), "Evidence of graphitic AB stacking order of graphite oxides", *J. Am. Chem. Soc.*, **130**, 1362-1366. <https://doi.org/10.1021/ja076473o>
- Johra, F.T., Lee, J.W. and Jung, W.G. (2014), "Facile and safe graphene preparation on solution based platform", *J. Ind. Eng. Chem.*, **20**, 2883-2887. <https://doi.org/10.1016/j.jiec.2013.11.022>
- Kang, J., Shin, D., Bae, S. and Hong, B.H. (2012), "Graphene transfer: Key for applications", *Nanoscale*, **4**, 5527-5537. <https://doi.org/10.1039/c2nr31317k>

- Kim, B.H., Hong, S.J., Baek, S.J., Jeong, H.Y., Park, N., Lee, M., Lee, S.W., Park, M., Chu, S.W., Shin, H.S., Lim, J., Lee, J.C., Jun, Y. and Park, Y.W. (2012), "N-type graphene induced by dissociative H₂ adsorption at room temperature", *Sci. Rep.*, **2**, 1-6. <https://doi.org/10.1038/srep00690>
- Kwan, Y.C.G., Ng, G.M. and Huan, C.H.A. (2015), "Identification of functional groups and determination of carboxyl formation temperature in graphene oxide using the XPS O 1s spectrum", *Thin Solid Films*, **590**, 40-48. <https://doi.org/10.1016/j.tsf.2015.07.051>
- Lee, Y., Bae, S., Jang, H., Jang, S., Zhu, S.-E., Sim, S.H., Song, Y. Il, Hong, B.H. and Ahn, J.-H. (2010), "Wafer-Scale Synthesis and Transfer of Graphene Films", *Nano Lett.*, **10**, 490-493. <https://doi.org/10.1021/nl903272n>
- Li, X., Cai, W., An, J., Kim, S., Nah, J., Yang, D., Piner, R., Velamakanni, A., Jung, I., Tutuc, E., Banerjee, S.K., Colombo, L. and Ruoff, R.S. (2009a), "Large-area synthesis of high-quality and uniform graphene films on copper foils", *Science*, **324**, 1312-1314. <https://doi.org/10.1126/science.1171245>
- Li, X., Zhu, Y., Cai, W., Borysiak, M., Han, B., Chen, D., Piner, R.D., Colomba, L. and Ruoff, R.S. (2009b), "Transfer of large-area graphene films for high-performance transparent conductive electrodes", *Nano Lett.*, **9**, 4359-4363. <https://doi.org/10.1021/nl902623y>
- Liang, X., Sperling, B.A., Calizo, I., Cheng, G., Hacker, C.A., Zhang, Q., Obeng, Y., Yan, K., Peng, H., Li, Q., Zhu, X., Yuan, H., Hight Walker, A.R., Liu, Z., Peng, L.M. and Richter, C.A. (2011), "Toward clean and crackless transfer of graphene", *ACS Nano*, **5**, 9144-9153. <https://doi.org/10.1021/nn203377t>
- Lin, Y.C., Jin, C., Lee, J.C., Jen, S.F., Suenaga, K. and Chiu, P.W. (2011), "Clean transfer of graphene for isolation and suspension", *ACS Nano*, **5**, 2362-2368. <https://doi.org/10.1021/nn200105j>
- Lindvall, N., Kalabukhov, A. and Yurgens, A. (2012), "Cleaning graphene using atomic force microscope", *J. Appl. Phys.*, **111**, 064904. <https://doi.org/10.1063/1.3695451>
- Liu, N., Chortos, A., Lei, T., Jin, L., Kim, T.R., Bae, W.G., Zhu, C., Wang, S., Pfattner, R., Chen, X., Sinclair, R. and Bao, Z. (2017), "Ultrasensitive and stretchable graphene electrodes", *Sci. Adv.*, **3**, 1700159. <https://doi.org/10.1126/sciadv.1700159>
- Mavrikakis, M. and Barteau, M.A. (1998), "Oxygenate reaction pathways on transition metal surfaces", *J. Mol. Catal. A Chem.*, **131**, 135-147. [https://doi.org/10.1016/S1381-1169\(97\)00261-6](https://doi.org/10.1016/S1381-1169(97)00261-6)
- Narayanaswamy, V., Obaidat, I.M., Kamzin, A.S., Latiyan, S., Jain, S., Kumar, H., Srivastava, C., Alaabed, S. and Issa, B. (2019), "Synthesis of graphene oxide-Fe₃O₄ based nanocomposites using the mechanochemical method and in vitro magnetic hyperthermia", *Int. J. Mol. Sci.*, **20**, 3368. <https://doi.org/10.3390/ijms20133368>
- Novoselov, K.S. (2004), "Electric field effect in atomically thin carbon films", *Science*, **306**, 666-669. <https://doi.org/10.1126/science.1102896>
- Park, J.H., Jung, W., Cho, D., Seo, J.T., Moon, Y., Woo, S.H., Lee, C., Park, C.Y. and Ahn, J.R. (2013), "Simple, green, and clean removal of a poly(methyl methacrylate) film on chemical vapor deposited graphene", *Appl. Phys. Lett.*, **103**, 1-5. <https://doi.org/10.1063/1.4824877>
- Pimenta, M.A., Dresselhaus, G., Dresselhaus, M.S., Cañado, L.G., Jorio, A. and Saito, R. (2007), "Studying disorder in graphite-based systems by Raman spectroscopy", *Phys. Chem. Chem. Phys.*, **9**, 1276-1291. <https://doi.org/10.1039/b613962k>
- Pirkle, A., Chan, J., Venugopal, A., Hinojos, D., Magnuson, C.W., McDonnell, S., Colombo, L., Vogel, E.M., Ruoff, R.S. and Wallace, R.M. (2011), "The effect of chemical residues on the physical and electrical properties of chemical vapor deposited graphene transferred to SiO₂", *Appl. Phys. Lett.*, **99**, 2009-2012. <https://doi.org/10.1063/1.3643444>
- Qu, D., Li, F.Z., Zhang, H. Bin, Wang, Q., Zhou, T.L., Hu, C.F. and Xie, R.J. (2014), "Preparation of graphene nanosheets/copper composite by spark plasma sintering", *Adv. Mater. Res.*, **833**, 276-279. <https://doi.org/10.4028/www.scientific.net/AMR.833.276>
- Rai, K.B., Khadka, I.B., Kim, E.H., Ahn, S.J., Kim, H.W. and Ahn, J.R. (2018), "Influence of hydrophobicity on the chemical treatments of graphene", *J. Korean Phys. Soc.*, **72**, 107-110. <https://doi.org/10.3938/jkps.72.107>
- Reckinger, N., Felten, A., Santos, C.N., Hackens, B. and Colomer, J.F. (2013), "The influence of residual oxidizing impurities on the synthesis of graphene by atmospheric pressure chemical vapor deposition",

- Carbon*, **63**, 84-91. <https://doi.org/10.1016/j.carbon.2013.06.042>
- Schröder, E. (2013), "Methanol adsorption on graphene", *J. Nanomater.*, **2013**.
<https://doi.org/10.1155/2013/871706>
- Soin, N., Roy, S.S., Lim, T.H. and McLaughlin, J.A.D. (2011), "Microstructural and electrochemical properties of vertically aligned few layered graphene (FLG) nanoflakes and their application in methanol oxidation", *Mater. Chem. Phys.*, **129**, 1051-1057. <https://doi.org/10.1016/j.matchemphys.2011.05.063>
- Suk, J.W., Lee, W.H., Lee, J., Chou, H., Piner, R.D., Hao, Y., Akinwande, D. and Ruoff, R.S. (2013), "Enhancement of the electrical properties of graphene grown by chemical vapor deposition via controlling the effects of polymer residue", *Nano Lett.*, **13**, 1462-1467. <https://doi.org/10.1021/nl304420b>
- Taghioskoui, M. (2009), "Trends in graphene research", *Mater. Today*, **12**, 34-37.
[https://doi.org/10.1016/S1369-7021\(09\)70274-3](https://doi.org/10.1016/S1369-7021(09)70274-3)
- Thomsen, C. and Reich, S. (2000), "Double resonant raman scattering in graphite", *Phys. Rev. Lett.*, **85**, 5214-5217. <https://doi.org/10.1103/PhysRevLett.85.5214>
- Tiwari, S.K., Sahoo, S., Wang, N. and Huczko, A. (2020), "Graphene research and their outputs: Status and prospect", *J. Sci. Adv. Mater. Devices*, **5**, 10-29. <https://doi.org/10.1016/j.jsamd.2020.01.006>
- Wang, L., Song, Y., Wu, A., Li, Z., Zhang, B. and Wang, E. (2002), "Study of methanol adsorption on mica, graphite and ITO glass by using tapping mode atomic force microscopy", *Appl. Surf. Sci.*, **199**, 67-73.
[https://doi.org/10.1016/S0169-4332\(02\)00502-0](https://doi.org/10.1016/S0169-4332(02)00502-0)
- Wong, K.L., Chuan, M.W., Chong, W.K., Alias, N.E., Hamzah, A., Lim, C.S. and Tan, M.L.P. (2019), "Modeling of low-dimensional pristine and vacancy incorporated graphene nanoribbons using tight binding model and their electronic structures", *Adv. Nano Res., Int. J.*, **7**(3), 207-219.
<https://doi.org/10.12989/anr.2019.7.3.207>
- Wu, G., Tang, X., Meyyappan, M. and Lai, K.W.C. (2017), "Doping effects of surface functionalization on graphene with aromatic molecule and organic solvents", *Appl. Surf. Sci.*, **425**, 713-721.
<https://doi.org/10.1016/j.apsusc.2017.07.048>
- Zevedejani, M.K. and Beni, Y. (2020), "Effect of laminate configuration on the free vibration/buckling of FG Graphene/PMMA composites", *Adv. Nano Res., Int. J.*, **8**(2), 103-114.
<https://doi.org/https://doi.org/10.12989/anr.2020.8.2.103>